Solar Phys (2010) 263: 185–208
DOI 10.1007/s11207-010-9540-5

Energetic Particle Acceleration and Propagation in Strong CME-Less Flares

K.-L. Klein · G. Trottet · A. Klassen

Received: 27 October 2009 / Accepted: 2 March 2010 / Published online: 3 April 2010

Abstract Flares and coronal mass ejections (CMEs) contribute to the acceleration and propagation of solar energetic particles (SEP) detected in the interplanetary space, but the exact roles of these phenomena are yet to be understood. We examine two types of energetic particle tracers related with 15 CME-less flares that emit bright soft X-ray bursts (GOES X class): radio emission of flare-accelerated electrons and *in situ* measurements of energetic electrons and protons near 1 AU. The CME-less flares are found to be vigorous accelerators of microwave-emitting electrons, which remain confined in low coronal structures. This is shown by unusually steep low-frequency microwave spectra and by lack of radio emission from the middle and high corona, including dm – m wave type IV continua and metre-to-hectometre type III bursts. The confinement of the particles accelerated in CME-less flares agrees with the magnetic field configuration of these events inferred by others. Two events produced isolated metric type II bursts revealing coronal shock waves. None of the seven flares in the western hemisphere was followed by enhanced particle fluxes in the GOES detectors, but one, which was accompanied by a type II burst, caused a weak SEP event detected at SoHO and ACE. Three of the CME-less flares were followed within some hours by SEP-associated flares from the same active region. These SEP-producing events were clearly distinct from the CME-less ones by their association with fast and broad CMEs, dm – m wave radio emission, and intense DH type III bursts. We conclude that radio emission at decimetre and longer waves is a reliable indication that flare-accelerated particles have access to the high corona and interplanetary space. The absence of such emission can be used as a signal that no SEP event is to be expected despite the occurrence of a strong soft X-ray burst.

K.-L. Klein (✉) · G. Trottet
Observatoire de Paris, LESIA, CNRS-UMR 8109, 92195 Meudon, France
e-mail: ludwig.klein@obspm.fr

G. Trottet
e-mail: gerard.trottet@obsm.fr

A. Klassen
Institut für Experimentelle und Angewandte Physik, Christian-Albrechts-Universität, 24118 Kiel, Germany
e-mail: klassen@physik.uni-kiel.de

Keywords Corona, radio emission · Energetic particles, acceleration · Energetic particles, propagation · Flares, energetic particles · Flares, relation to magnetic field

1. Introduction

The acceleration of energetic electrons and ions that escape to the interplanetary space is a well-known manifestation of solar activity. But the origin of enhanced fluxes of solar energetic particles (SEP) detected in space is difficult to identify. This is because the events are usually associated with complex coronal activity. When the different observing conditions for the detection of flares and coronal mass ejections (CMEs) are taken into account, it turns out that large SEP events, routinely monitored by the *Geosynchronous Operational Environmental Satellites* (GOES) operated by NOAA, are associated with both fast and broad CMEs and flares, as seen, *e.g.*, by soft X-ray patrol observations (Cane, Erickson, and Prestage, 2002; Gopalswamy *et al.*, 2004). Statistical correlations of SEP parameters and the associated activity are ambiguous. For instance, there is some correlation between the SEP peak flux and the plane-of-the-sky speed of CMEs, but SEP fluxes can vary by several orders of magnitude for a given speed (Kahler, 2001; Gopalswamy *et al.*, 2004). Similarly, there is a more or less pronounced correlation between the peak fluxes of SEP and soft X-rays (Gopalswamy *et al.*, 2004), which is well improved when only SEP events in the western hemisphere are considered (Belov *et al.*, 2007). Chertok (1990) has also shown a clear correlation between SEP peak fluxes at energies above 10 MeV and the fluence of gamma-ray emission in the (4 – 7) MeV range, which is dominated by nuclear lines from accelerated protons and ions.

It appears that statistical correlations will not allow us to decide which role flares and CMEs actually play in SEP events. A useful approach to study particle acceleration and escape under well-defined conditions would be the identification of 'pure' events, *i.e.* fast CMEs without flares or powerful flares without CMEs. It was shown (Marqué, Posner, and Klein, 2006) that the few fast CMEs with no radio signature of flare-related particle acceleration did not produce conspicuous SEP events detected at Earth, even when they were well connected. The authors concluded that a CME shock alone was not a sufficient condition for an SEP event. Here we address the opposite question: do strong flares without CMEs produce SEP events? CME-less strong flares were identified by Wang and Zhang (2007) and Gopalswamy, Akiyama, and Yashiro (2009). In the present paper we analyse the associated manifestations of energetic electrons in the corona through the radio emission, and also investigate if the Earth-connected events are followed by energetic particles in space.

In Section 2 we briefly summarise the identification of CME-less flares (Section 2.1) by Wang and Zhang (2007) and Gopalswamy, Akiyama, and Yashiro (2009), present the associated radio emission from centimetre-to-hectometre wavelengths (Section 2.2), and search for SEP signatures in space (Section 2.3) using the GOES, SoHO and ACE spacecraft. In Section 3 we study SEP-associated flares that occurred a few hours after three of the CME-less flares in the same active region, and compare the radio properties of the two event types. The results are discussed in Section 4 with respect to the magnetic confinement of the flare-accelerated particles (Section 4.1). The origin of type II coronal shocks and their role in SEP acceleration is briefly addressed in Section 4.3. The relevance of the findings for SEP forecasting is alluded to in Section 4.4. A preliminary account of this research has been published by Klein, Trottet, and Vilmer (2009).

2. Radio Emission from CME-Less Flares

2.1. The Identification of CME-Less Flares

A set of CME-less strong flares, where the soft X-ray emission at the event peak exceeded 10^{-4} W m^{-2} (GOES X class), was identified by Wang and Zhang (2007). Flares that are not accompanied by a coronal mass ejection are usually called "confined". The denomination already presumes an explanation. We prefer the neutral term "CME-less" flare in this paper. Wang and Zhang (2007) considered a flare as CME-less when *i*) no CME lifted off – as inferred from the linear backward extrapolation of its time – height trajectory – within a 60 min window centred on the soft X-ray onset, *ii*) no EUV dimming was observed with the flare brightening. EUV dimmings are indeed statistically related with CMEs (Bewsher, Harrison, and Brown, 2008) and can be related to the outflow of material in the course of the CME (Jin *et al.*, 2009), although remarkable exceptions have also been reported (*e.g.*, Robbrecht, Patsourakos, and Vourlidas, 2009). Wang and Zhang (2007) found that eleven out of a total of 104 GOES X class flares during the last solar cycle (1996 – 2004) were not accompanied by CMEs.

Another list of CME-less flares was compiled by Gopalswamy, Akiyama, and Yashiro (2009). They used a slightly different method, as described in Yashiro *et al.* (2008): X class flares were identified where no CME was listed within a window of ± 1.5 hrs around the flare onset in the SoHO/LASCO CME catalogue (http://cdaw.gsfc.nasa.gov/CME_list/index.html) of Yashiro *et al.* (2004). Then presumably false associations were eliminated by visual inspection of the LASCO and EIT movies. These authors identified 13 CME-less X class flares between 1996 and 2005.

The selection criteria of CME-less flares differ slightly between the two papers, but nine events are common to the two lists. The combined list of 15 CME-less X class flares is displayed in Table 1. Column 1 gives the date, start time and importance of the GOES soft X-ray burst and the location of the associated flare, from Wang and Zhang (2007), Gopalswamy, Akiyama, and Yashiro (2009), and *Solar Geophysical Data – Comprehensive Reports* published by NOAA. The events only contained in the list of Wang and Zhang (2007) are labelled "W" (end of col. 1), those only contained in the list of Gopalswamy, Akiyama, and Yashiro (2009) are labelled "G".

The events on 09 June 2003 and 16 July 2004, 13:49 UT were not retained by Gopalswamy, Akiyama, and Yashiro (2009). These authors justified the exclusion of the latter event by the identification of an uncatalogued CME. But this CME was already in the LASCO field of view beyond 2.5 $R_\odot$ at the time of the start of the soft X-ray burst, which shows that it lifted off well before the flare. The 09 June 2003 event occurred during a very active period of the solar corona, as shown by the daily SoHO/LASCO difference movies and also by Figure 1 of Wang and Zhang (2007). However, the CME identified in the LASCO images at the time of the flare started several hours earlier, and no EUV dimming was seen by SoHO/EIT with this flare (Zhang, personal communication). So the inclusion in the event list is consistent with the selection criteria. Several events of Gopalswamy, Akiyama, and Yashiro (2009) were not considered by Wang and Zhang (2007): 25 November 2001, 31 October 2002, and the two events of 2005 (15 January, 15 September) that were not within the time frame used by Wang and Zhang (2007). We analyse in the following all events of Table 1.

2.2. Characteristics of the Radio Emission

Information on the microwave emission was derived from the patrol data especially of the RSTN network (observing frequencies: 15.4, 8.8, 4.995, 2.695, 1.415, 0.610, 0.410 and

Table 1 Radio emission from CME-less flares.

Flare	Microwaves				dm-m-λ	Type	DH
	CO(HF) [GHz]	Peak	CO(LF) [GHz]	$\alpha_{lf}(\nu_1, \nu_2)$		II	III
(1)	(2)	(3)	(4)	(5)	(6)	(7)	(8)
2000							
06 June 13:30 X1.1 N20 E14	>15	13:32/9 – 15 GHz/∼400 sfu	–	–	noise storm	no	no
30 September 23:13 X1.2 N07 W90	>80	23:19/≥35 GHz/5000 sfu	2.0 – 1.0	5.1 (2.0, 3.7)	noise storm ?	no	no
2001							
02 April 10:04 X1.4 N16 W60	>50	10:07/15 GHz/1200 sfu	–	–	noise storm	no	no
23 June 04:02 X1.2 N10 E23	35 – 17	04:08/9.4 GHz/100 sfu	<1	1.7 (1.0, 2.0)	noise storm ?	no	no
25 November 09:51 X1.1 S16 W69 G	>35	09:49/∼15.4 GHz/ ∼150 sfu	–	–	quiet	no	late
2002							
31 October 16:52 X1.2 N29 W90 G	>15	16:51/8.8 GHz/3400 sfu	2.7 – 1.4	4.2 (2.7, 5.0)	III ≤245 MHz	no data	yes
2003							
09 June 21:31 X1.7 N12 W33 W	>35	21:37/15 – 17 GHz/870 sfu	1.4 – 0.6	2.0 (1.0, 2.0)	II precursor >400 MHz	II F/H 360 – 30 MHz	no
2004							
26 February 01:50 X1.1 N14 W15	>35	01:55/9.4 GHz/580 sfu	3.7 – 1.0	5.8 (2.0, 3.7)	noise storm	no	no
15 July 18:15 X1.6 S11 E45	>15	18:23/≥15 GHz /1900 sfu	1.4 – 0.6	2.5 (1.4, 2.7)	noise storm	no	no
16 July 01:43 X1.3 S11 E41	>35	02:03/17 GHz/1600 sfu	1.4 – 0.6	4.0 (1.0, 2.0)	noise storm	no	no
16 July 10:32 X1.1 S10 E36	>35	10:39/>15 GHz/470 sfu	1.4 – 0.6	2.0 (1.4, 2.7)	noise storm	no	no
16 July 13:49 X3.6 S10 E36 W	>35	13:54/9 – 15 GHz/6800 sfu	1.4 – 0.6	4.2 (1.4, 2.7)	noise storm	55 – 40 MHz	no
17 July 07:51 X1.0 S11 E25	>15	07:57 ≥15 GHz/840 sfu	1.4 – 0.6	3.2 (1.4, 2.7)	noise storm	no	no
2005							
15 January 00:22 X1.2 N11 E10 G	>35	00:41/17 – 35 GHz/4400 sfu	2.7 – 0.6	4.0 (3.7, 9.4)	noise storm	no	no
15 September 08:38 X1.1 S12 W14 G	>15	08:36/≥15 GHz/3900 sfu	1.4 – 0.6	4.4 (1.4, 2.7)	noise storm	no	no

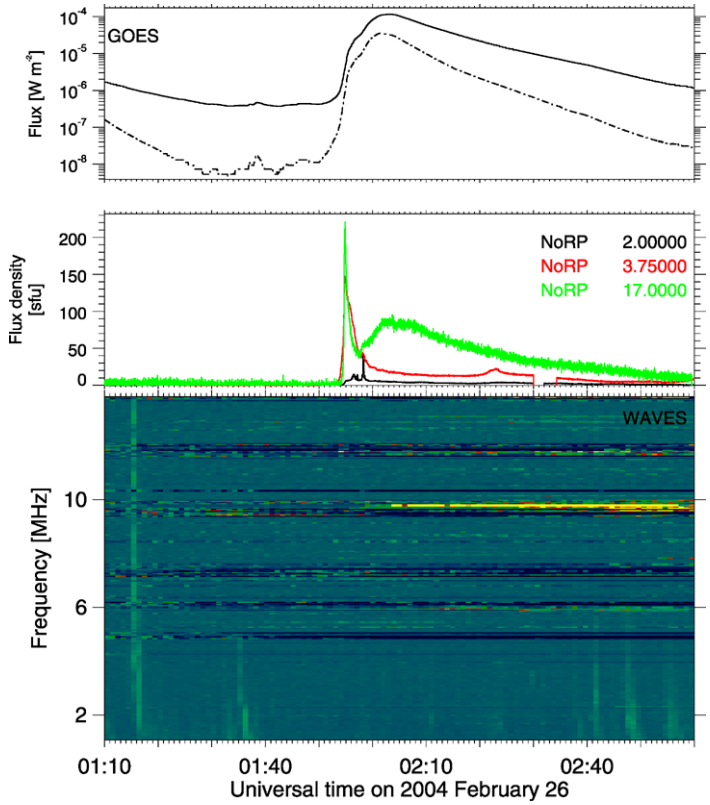

Figure 1 Time history of the soft X-ray (top panel; GOES – solid line 0.1 – 0.8 nm, dashed-dotted line 0.05 – 4 nm, respectively), microwave (middle; Nobeyama Radio Polarimeter, NoRP; frequencies listed in units of GHz) and decametre-to-hectometre (DH) wave emission (bottom; *Wind*/WAVES) around the CME-less GOES X class flare on 26 February 2004 01:50 UT.

0.245 GHz, provided by NGDC/WDC Boulder[1]) and the Nobeyama Radio Polarimeter[2] with observing frequencies 80, 35, 17, 9.4, 3.75, 2.0, 1.0 GHz (Nakajima *et al.*, 1985). Most of the data were available on line. In some events data from the University of Bern patrol observations (courtesy A. Magun) were also used.

A representative example of the soft X-ray and radio time histories of CME-less flares is shown in Figure 1. The soft X-ray burst (top panel) has a rapid rise, on which a second event may be superposed shortly before the peak. The microwave emission at 3.75 and 17 GHz shows a pronounced impulsive peak during this phase, followed by a monotonical decay at 3.75 GHz and a new, more gradual rise, probably of thermal origin, at the higher frequency. The weak counterpart at 2 GHz has a different time profile, and no event was seen at 1 GHz (not shown here). This suggests that the microwave spectrum is cut off somewhere between 1.0 and 3.75 GHz. The bottom panel of Figure 1 displays the decametre-to-hectometre (DH) wave spectrum (14 – 1 MHz). The type III bursts shown by the nearly vertical light blue traces are produced by electron beams that travel through the high corona

[1] http://www.ngdc.noaa.gov/stp/SOLAR.

[2] http://solar.nro.nao.ac.jp/norp/.

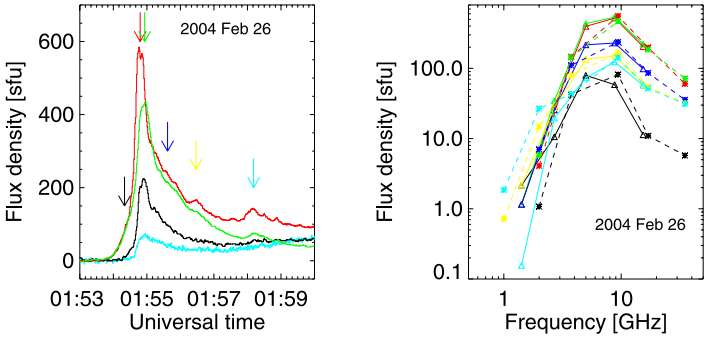

Figure 2 Left: Time history of the microwave emission (RSTN/Learmonth: green 4.995 GHz, black 15.4 GHz; Nobeyama Radio Polarimeter – NoRP: red 9.4 GHz, light blue 35 GHz) during the 26 February 2004 01:50 UT flare. Right: Flux density spectra at selected times, as indicated by the arrows in the left figure. RSTN measurements are connected by solid lines, NoRP data by short-dashed lines.

(typically $3-10\ \mathrm{R}_\odot$ in this frequency range). Type III bursts in this range will be referred to as DH type III bursts in the following. A key feature of this and other CME-less flares is that no DH type III burst is detected during the impulsive flare phase, at the time of the pronounced peak of the microwave emission.

The microwave time history during the impulsive flare phase is shown in more detail in the left hand panel of Figure 2. Flux density spectra at selected times during the event are plotted in the right panel. The spectrum has a well-defined and rather steep rise ($\sim\nu^{5.8}$) at low frequencies to a maximum near 9 GHz. The low-frequency cutoff and steep spectrum are again typical features of these CME-less flares, as will be shown below.

The radio characteristics of the entire set of CME-less X class flares are listed in Table 1. Parameters of the microwave spectrum at the maximum of the event are listed in columns 2–5. In the events of 06 June 2000, 02 April and 25 November 2001, where no data were available on line, the information in the table is quoted from RSTN observations reported in *Solar Geophysical Data – Comprehensive Reports*. Columns 2 and 4 give the extension of the microwave spectrum towards high and low frequencies, respectively. The high-frequency cutoff CO(HF) is only a rough indication, because most often the event was seen at all frequencies of patrol observations, depending on the available instruments: the Nobeyama Radio Polarimeter also monitors the Sun at 80 GHz, and Bern at 50 GHz, whereas the highest frequency of RSTN is 15.4 GHz. The low-frequency limits CO(LF) were easier to identify. Column 4 gives the lowest frequency where the microwave burst was detected, and the subsequent lower frequency where it was not seen. Column 3 relates the time, frequency and flux density of the maximum of the microwave burst. The flux density is the value after subtraction of the pre-event background. It is given in solar flux units ($1\ \mathrm{sfu} = 10^{-22}\ \mathrm{W\,m^{-2}\,Hz^{-1}}$). Column 5 gives the spectral index of the low-frequency microwave spectrum, computed between the two frequencies within parentheses.

Columns 6 and 7 contain a brief description of the decimetre-to-metre wave emission, which here means frequencies from about 600 MHz to the ionospheric cutoff near 30 MHz. The information was derived from catalogues and quick look plots at the web sites of different radio observatories (Table 2), and from inspection of RSTN single frequency records, when available. In one case the emission was that of the quiet corona, because no isolated source was seen in images of the Nançay Radioheliograph (NRH; Kerdraon and Delouis, 1997). Most often a noise storm was observed, as is common in periods of high solar activity. Noise storms are time-extended (hours to days), flare-independent dm-m wave radio

Table 2 Decimetre-to-metre wave radio observatories.

Observatory and homepage	Frequency range [MHz]
Phoenix-2, ETH Zurich (Messmer, Benz, and Monstein, 1999) www.astro.phys.ethz.ch/catalog/catalog_nf.html	4000 – 100
Tremsdorf Observatory, AI Potsdam (OSRA; Mann *et al.*, 1992) www.aip.de/groups/osra/	800 – 40
ARTEMIS, University of Athens (Caroubalos *et al.*, 2001) www.cc.uoa.gr/artemis/	650 – 20
IZMIRAN Moscow helios.izmiran.rssi.ru/lars/LARS.html	270 – 25
Nançay Decametric Array (NDA; Lecacheux, 2000) www.obs-nancay.fr/a_index.htm	70 – 20
Green Bank Radio Spectrograph (GBSRBS; White, 2007) gbsrbs.nrao.edu/	70 – 18
Hiraiso Radio Spectrograph (HiRAS) sunbase.nict.go.jp/solar/denpa/index.html	2500 – 25
Culgoora Radio Spectrograph (Type II list) www.ips.gov.au/Solar/2/6/1	1800 – 18

emissions associated with active regions. Whether or not this is the active region where the CME-less flare occurred cannot be decided without imaging observations. When a noise storm was clearly seen by the NRH a few hours from the CME-less flare, and no other reliable data source was available, the dm – m emission during the flare was qualified as a noise storm with a question mark. In two events flare-related radio emission was observed: a type III burst and a type II burst with a precursor. The presence or absence of a metric type II burst is noted in column 7.

Column 8 reports the detection or not of a type III burst at decametric-to-hectometric wavelengths (frequency range 14 – 1 MHz) with the WAVES spectrograph aboard the *Wind* spacecraft (Bougeret *et al.*, 1995). The digital data were plotted and compared with the soft X-ray and microwave time profiles. A complication arises because noise storms at metre wavelengths are often associated with storms of DH type III bursts. Storm type III bursts are usually faint and occur in uninterrupted series during several hours or more (Kai, Melrose, and Suzuki, 1985; Kayser *et al.*, 1987), while flare-related DH type III bursts occur during the impulsive phase, characterised by the rise of the soft X-ray flux and bright microwave emission. Since they are not flare-related, storm type III bursts were not marked in the Table. This ambiguity will be addressed again in the Discussion (Section 4.1).

We now proceed to summarise the results of Table 1.

2.2.1. Centimetre Wave Bursts

In order to put the microwave emission of the CME-less X class flares into the broader context, we compare the results with those of two statistical studies: that of 412 microwave bursts observed during the years 2001 and 2002 with the small antennas of the Owens Valley Solar Array with excellent frequency coverage in the 1.2 – 18 GHz range (Nita, Gary, and Lee, 2004), and the study of Guidice and Castelli (1975) of more than 2400 bursts at RSTN

frequencies (and 35 GHz) between 1968 and 1971. In both papers a distinction was made between pure centimetric spectra, referred to as "C class", pure decimetric spectra, and combined cm and dm spectra.

The CME-less bursts of Table 1 are among the pure centimetric events. The lowest frequency where the microwave bursts were detected was 1.4 GHz in cases where we could analyse the data in detail (*i.e.* all events but 06 June 2000, 02 April 2001, 25 November 2001).

2.2.1.1. Peak Flux Density

- The peak flux densities of the CME-less flares range between 100 and 6800 sfu. Six of the 12 events have peak flux densities above 1900 sfu.
- In the sample of Nita, Gary, and Lee (2004) the median peak flux density is 52 (-26, $+85$) sfu (the $\pm$values indicate the range of values comprising 50% of the events). In pure cm spectra the median peak flux is 46 (-22, $+59$) sfu, in the centimetric component of two-component spectra (*i.e.* where also a dm component was detected) the median is much higher: 98 (-47, $+373$) sfu. Guidice and Castelli (1975) showed that only 20% of the microwave bursts with pure cm spectra have peak flux density above 50 sfu, and 3% above 500 sfu.

Clearly the peak flux densities measured during the CME-less flares are much higher than in average microwave bursts. This is at least partly due to our selection of strong soft X-ray bursts, because there is an overall correlation between the average flux density of microwave bursts and the average flux of soft X-ray bursts (Benz and Güdel, 1994), as well as between the peak values of the two emissions (Spangler and Shawhan, 1974). But while soft X-rays are of thermal origin, the conclusion here is that the studied flares give rise to strong electron acceleration to mildly relativistic energies.

2.2.1.2. Peak Frequency

- The peak frequency of the CME-less flares ranges between 8.8 and more than 35 GHz. Seven of the 12 events have peak frequencies above 15 GHz.
- In the sample of Nita, Gary, and Lee (2004) the median peak frequency is 6.6 GHz (-1.7, $+2.4$). It is well known (Fürst, 1971; Guidice and Castelli, 1975), and confirmed by Nita, Gary, and Lee, that the bulk of the emission shifts to higher frequencies as peak flux increases. The highest peak frequency found by Nita, Gary, and Lee (2004) was 9.0 GHz (-3.5, $+3.5$) in the case of the pure centimetric events with peak flux densities above 1000 sfu. Their sample extends to 18 GHz. Correia, Kaufmann, and Magun (1994) showed that 25% of the radio bursts that are observable at 19 and 35 GHz have peak frequencies above 19 GHz.

The peak frequencies measured during the CME-less flares are significantly higher than those of average bursts, even if one restricts oneself to microwave bursts with peak flux density above 1000 sfu. Since the microwave radiation comes from the gyrosynchrotron mechanism, this finding supports high numbers of energetic electrons and sources with strong magnetic fields, in line with the high peak fluxes.

2.2.1.3. Low-Frequency Spectral Index

- The low-frequency spectral index of the CME-less X class flares ranges between 1.7 and 5.8. Eight of the 12 events have a spectrum that is steeper than $\nu^{2.5}$, which is the slope of the self-absorbed synchrotron spectrum emitted by ultrarelativistic electrons in

a uniform magnetic field. The spectrum is a little steeper for gyrosynchrotron emission from mildly relativistic electrons, depending on the spectral index of the energy spectrum of the radiating electrons (*cf.* eq. 37 of Dulk, 1985). Six of the 12 CME-less events have a low-frequency spectral index between 4.0 and 5.8.

- In the sample of Nita, Gary, and Lee (2004) the median low-frequency spectral index is found to be 1.8 (-0.5, $+1.0$) for the whole sample of cm components, a little flatter (1.6) in the sample with both cm and dm components. The spectra become flatter as the peak flux density increases.

The low-frequency spectra of the microwave bursts in CME-less flares are significantly steeper than those of an average sample, and also much steeper than the slope predicted for uniform self-absorbed gyrosynchrotron spectra. Such steep low-frequency spectra can be explained by Razin suppression of gyrosynchrotron radiation, which requires a dense plasma. Since the frequency below which Razin suppression becomes noticeable is roughly $20n_e/B$ (n_e: ambient electron density, B: magnetic field strength; cgs units) (eq. 4.10 of Pacholczyk, 1970), and since the high peak frequencies of the CME-less flares suggest emission from relatively strong fields, Razin suppression requires high thermal electron densities. With the above expression: $n_e > 3 \times 10^{10} \frac{\nu}{2\ \mathrm{GHz}} \frac{B}{300\ \mathrm{G}}\ \mathrm{cm}^{-3}$ in order that Razin suppression operates at frequency ν. Given that the steep spectra are observed in the range of a few GHz, a radio source with ambient density well above $10^{10}\ \mathrm{cm}^{-3}$ is required, which can only be located in compact loops in the low corona.

2.2.2. *Bursts at Decimetre-to-Hectometre Wavelengths*

The confinement of flare-accelerated electrons in low coronal structures is confirmed by the absence of flare-associated radiation at decimetric and longer wavelengths: 12 out of 15 CME-less flares displayed no related dm – m wave emission, and 13 out of 15 were not accompanied by a DH type III burst. We now look in more detail into the events that display radio emission at decimetric and longer wavelengths, to check if they contradict the confinement of the flare-accelerated electrons.

2.2.2.1. Type III Emission at Metric-to-Hectometric Wavelengths DH type III bursts were seen by the WAVES spectrograph during the soft X-ray bursts on 25 November 2001 and 31 October 2002. On 25 November 2001 the type III burst occurred after the soft X-ray maximum. It is labelled "late" in Table 1. The timing of the different emissions in the 31 October 2002 burst is shown in Figure 3. The 245 MHz emission (middle panel) appears as the high-frequency counterpart of the DH type III burst, but occurred in the decay phase of the microwave burst. This time delay shows that the type III emission does not trace electrons escaping directly from the microwave source. The escaping electrons are rather accelerated independently. The disconnection between microwave and metre wave emission is further supported by the absence of burst signatures at 410 MHz and by the steep low-frequency spectrum of the microwave burst (Table 1). We can therefore sharpen our earlier statement: none of the microwave bursts had a simultaneous type III burst at metre and longer waves that would have signalled the escape of electrons from the microwave source to the high corona or the common acceleration of microwave producing and escaping electrons.

2.2.2.2. Radio Bursts from Coronal Shock Waves Two of the CME-less flares were accompanied by coronal shocks as shown by metre-wave type II bursts. One (16 July 2004, 13:49 UT) was restricted to a narrow range of low frequencies. But the type II burst of 09 June 2003 had a broad frequency extent and a well-defined spectral structure, with a

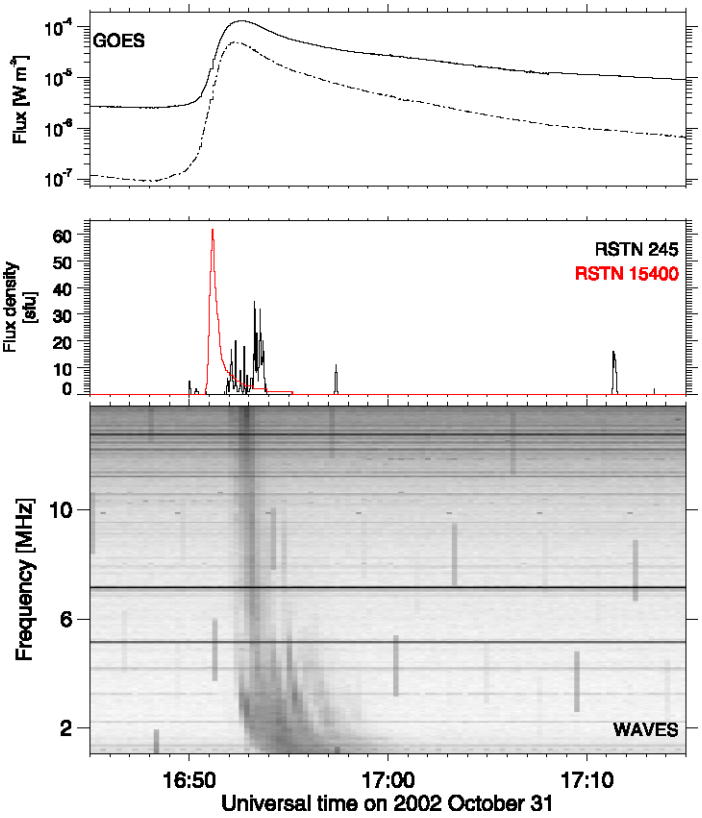

Figure 3 Time history of the soft X-ray (top panel; GOES), microwave (middle; RSTN/Sagamore Hill 0.245 and 15.4 GHz; flux density at 15.4 GHz multiplied by 0.03) and decametre-to-hectometre (DH) wave emission (bottom; *Wind*/WAVES) around the CME-less GOES X class flare on 31 October 2002 at 16:52 UT.

fundamental and a harmonic lane (Figure 4). Since, as we will see below, this flare was followed by a minor SEP event, we discuss the observation of the type II burst in some detail. The WAVES spectrograph detected a DH type III burst, which started between 21:45 and 21:46 UT at 14 MHz, *i.e.* during the metric type II burst.

The harmonic lane of the type II burst is split into two bands. If this band splitting is interpreted as a signature of simultaneous emission from both downstream and upstream of the shock (Vršnak *et al.*, 2001), the frequency ratio of the split bands reflects the density compression ratio at the shock. This ratio is in the range 1.2 – 1.3 on 09 June 2003, implying a compression ratio of about 1.6. This corresponds to an Alfvenic Mach number $M_A = 1.5$, if the plasma has low beta, and 2 for $\beta = 1$, in the case of a perpendicular shock (after Eq. 5.35 of Priest, 1982). The fast magnetosonic Mach number is 1.4 – 1.5. The compression ratio places this peculiar shock in the subcritical regime for a plasma beta below about 0.4 (Mann, Classen, and Aurass, 1995).

We estimate the exciter speed under the hypothesis that the type II burst source travels radially outward through a hydrostatically structured corona. This hypothesis may be questioned (*cf.* discussions in Nelson and Robinson, 1975; Gergely, Kundu, and Hildner, 1983; Gergely *et al.*, 1984; Klein *et al.*, 1999, 2003; Dauphin, Vilmer, and Krucker, 2006), but is widely used. The two split bands of the harmonic type II lane have a relative drift rate in

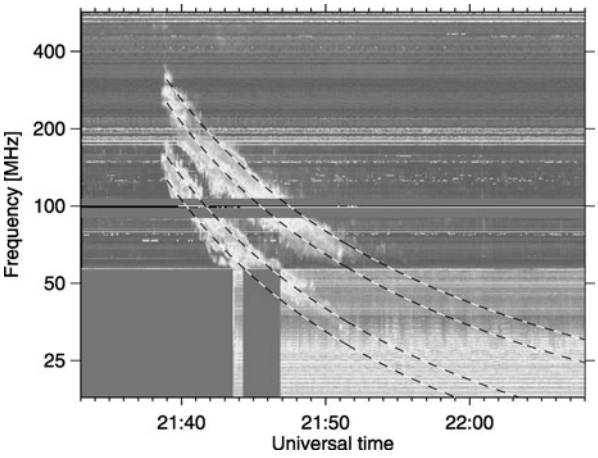

Figure 4 Dynamic spectrum (Culgoora Radio Observatory) of the type II burst on 09 June 2003. The dashed lines show two split bands of the fundamental and harmonic lane, for the model of an exciter moving outward at speed 606 km s^{-1} through a hydrostatically stratified plasma. The parameters of the model are: $T = 1.4$ MK, heliocentric distance of the harmonic level at 130 MHz 1.5 R$_\odot$, frequency ratio of the split bands 1.23.

the vicinity of 130 MHz of $\frac{\Delta \ln \nu}{\Delta t} = -1.93 \times 10^{-3}$ s^{-1}. In a hydrostatic isothermal density model, *i.e.* an exponential law in the vicinity of the heliocentric distance r_0, this implies an exciter speed of

$$\upsilon = 195 \frac{T}{1\ \mathrm{MK}} \left(\frac{r_0}{R_\odot} \right)^2 \mathrm{km\,s^{-1}}. \quad (1)$$

If the heliocentric distance of the level of harmonic emission at 130 MHz is assumed at r_0 in the range (1.2 – 1.5) R$_\odot$, and the temperature is 1.4 MK like in the Newkirk density model (see also Koutchmy, 1994), the exciter speed is about 390 – 610 km s^{-1}. An example of such a fit is shown by the four dashed (black and white) lines in Figure 4. They represent the fundamental and harmonic lane (frequency ratio 1:2) with the respective split bands, supposed to have a frequency ratio of 1.23. The low exciter speed is in line with the low Mach number derived above.

In conclusion, the two events with type II bursts are again consistent with the confinement of flare-accelerated electrons in low coronal structures, while the coronal shocks accelerate electrons in different regions. The association of the type II burst with a DH type III burst suggests that electrons escape to interplanetary space from the coronal shock on 09 June 2003.

2.3. A Search for SEP Signatures in CME-Less Flares

Seven of the CME-less X class flares occurred in the western solar hemisphere. If energetic particles were released to interplanetary space, they would be expected to be detected by spacecraft in Earth orbit (*e.g.*, GOES) or at the Sun-Earth Lagrange point (*e.g.*, SoHO and ACE). But the plots of GOES proton fluxes at energies above 10, 50 and 100 MeV (provided with the CME catalogue at http://cdaw.gsfc.nasa.gov/CME_list/index.html) show no SEP event for any of the flares.

We evaluated the background and standard deviation of the GOES 5 min proton fluxes in the energy channel above 10 MeV during several hours after the soft X-ray burst (2 hrs on 2 April 2001, 4 hrs during the other events where the GOES SEP signal was at its background level). The data are provided by OMNIWeb at NASA *Goddard Space Flight Center* (http://omniweb.gsfc.nasa.gov/html/omni_source.html#flu). The upper limit of the GOES proton intensity, taken as three standard deviations above background, is given in column 2

Table 3 A search for SEP in CME-less flares from the western hemisphere.

Flare	GOES	SoHO/CoSTEP	
	p(≥10 MeV) [pfu]	e(≥200 keV)	p(≥4.3 MeV)
(1)	(2)	(3)	(4)
2000			
30 September 23:13	<0.2 (9)	faint	none
2001			
02 April 10:04	<1 (10)	previous/none	previous/none
25 November 09:51	previous (7)	previous/none	previous/none
2002			
31 October 16:52	<0.9 (6)	rise previous/none	rise previous/none
2003			
09 June 21:31	<0.3 (12)	previous/excess	previous/excess
2004			
26 February 01:50	<0.3 (7)	none	(CIR)
2005			
15 September 08:38	previous (5)	previous/none	previous/none

of Table 3 in particle flux units (1 pfu = 1 $cm^{-2}\,s^{-1}\,sr^{-1}$). The value within parentheses is the expected value, estimated with the empirical relationship that Garcia (2004 his Eq. 6) derived between proton peak intensities in space and parameters of the associated soft X-ray burst:

$$\log \Phi_{10} = 2.34(\log \mathrm{EM} - 49.432) - 0.1055 P_X + 0.44 \Delta t. \quad (2)$$

Φ_{10} is the proton intensity integrated over all energies above 10 MeV, in pfu. EM is the soft X-ray emission measure in units of cm^{-3}, P_X the peak flux in the (0.1 – 0.8) nm channel, in units of 10^{-4} $W\,m^{-2}$, and Δt the time lapse in hours between the onset of the X-ray burst and the time when the flux has decayed to 25% of its maximum level in the (0.05 – 0.4) nm channel. The emission measure was evaluated using standard software available in the *SolarSoft*[3] package, based on version 6.0.1 of the *Chianti* model. It appears that a weak, but significant GOES SEP event would be expected in association with these flares, but that none was detected in five of the seven events.

The analysis is difficult in the two other cases, where the flare occurred during the decay of a previous SEP event. No new injection on top of the decay was found in the 15 September 2005 event. The situation is more ambiguous on 25 November 2001, where minor fluctuations occurred on top of the decaying count rate in the GOES detector channels above, respectively, 10 and 50 MeV, shortly after the flare. However, they show no indication of a velocity-dependent start, which argues against the interpretation in terms of a fresh solar particle release.

We checked this result with the electron and low-energy proton measurements of SoHO/CoSTEP and ACE/EPAM. Columns 3 and 4 of Table 3 show the results of inspection of the CoSTEP data (Müller-Mellin *et al.*, 1995) for electrons at energies above 0.25 MeV

[3] http://www.lmsal.com/solarsoft/.

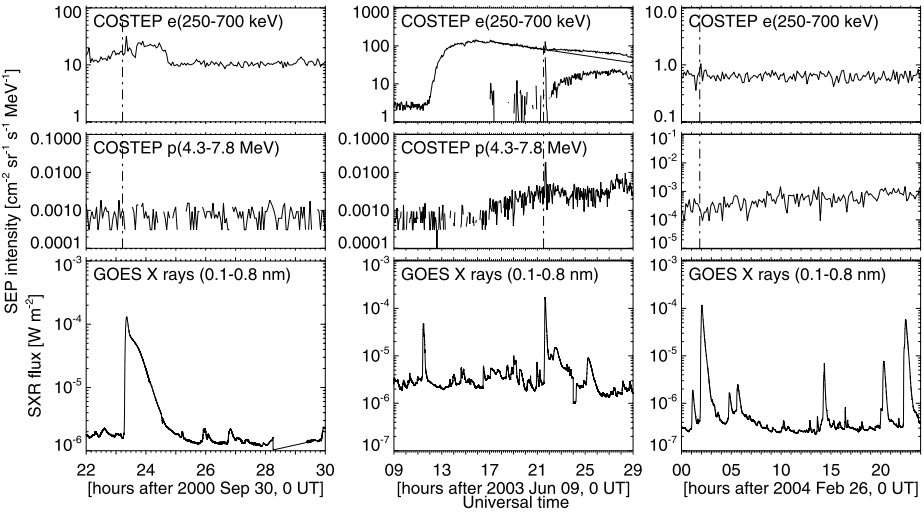

Figure 5 Time histories of soft X-ray flux (GOES) and particle intensities (SoHO/CoSTEP) during three CME-less flares. In the top figure of the middle panel (09 June 2003) the original electron intensity is plotted together with the exponential fit to the measurements between 17 UT and 21 UT (dashed-dotted line) and the difference between the original intensity and this fit. Dashed-dotted vertical lines in the top and middle panels indicate the start time of the CME-less soft X-ray burst.

and protons above 4.3 MeV. The same results are obtained by ACE/EPAM (Gold *et al.*, 1998). In all but two cases the background near the time of the CME-less flare was enhanced by the decaying (in one case rising) count rate produced by a previous event. In four cases no new particle injection is discernible in conjunction with the CME-less flare. In the three other cases there are indications for faint enhancements of the particle intensities following the flare. The CoSTEP intensity – time histories of electrons (250 – 750 keV) and protons (4.3 – 7.8 MeV) are plotted in Figure 5. The SEP intensities plotted in the top and middle panels may show a spike at the time of the soft X-ray burst. This spike is not due to particles, but is produced by X-ray photons at energies $\geq$30 keV. An enhanced intensity in electrons above 250 keV is detected on 30 September 2000 and 09 June 2003, and enhanced intensity of protons on 09 June 2003 and 26 February 2004. The travel time of these particles along an interplanetary path of 1.2 AU, similar to the length of a standard Parker spiral, is between 11 and 13 min for the electrons in the (250 – 700) keV range, and 1.5 hr for the low-energy protons.

- On 30 September 2000 the electron intensity rose rather abruptly near 23:40 UT, stayed on a roughly constant level, and decreased abruptly about an hour later. The time profile is not that of a typical electron event with a rapid rise and slow decay. ACE magnetic field data[4] show successive opposite rotations that give evidence of interacting ICMEs (P. Démoulin, personal communication). Since both ACE and SoHO are located near the Lagrangian point (L1), the magnetic field configuration is similar at both spacecraft. One may therefore suspect that the electron intensity enhancement is not the effect of a solar acceleration related to the CME-less flare.

[4] http://www.srl.caltech.edu/ACE/ASC/DATA/level3/summaries.html.

- During the 09 June 2003 event (central column in Figure 5) the new electron release shows up as a reduced rate of decay of the SEP intensity from the previous event. We represented the decay between 17 and 21 UT by an exponential and subtracted this fit from the time profile after 17 UT. The difference time profile is the lower curve in the top middle panel of Figure 5. It shows indeed a rise of the electron intensity shortly after the flare. A few hours later a new rise is also seen in the proton intensities above 4 MeV. These time profiles are consistent with a weak SEP event associated with the flare.
- On 26 February 2004 (right column of Figure 5) the soft X-ray flare was followed by a very slow and faint rise of the proton intensity, which is hardly perceptible in the figure, but continued until a shallow maximum on 29 February. Along with the particle enhancement ACE solar wind instruments observed a gradual increase of the solar wind speed from about 300 to 700 km s^{-1} and of the magnetic field intensity, and a change of the magnetic field direction. A particle increase with a similar time profile had been observed in the previous solar rotation by ACE and CoSTEP. This particle enhancement is hence related to a corotating interaction region at the interface between a slow and a fast solar wind stream, not to the CME-less flare.

Altogether the CoSTEP and EPAM observations confirm that the CME-less flares do in general not generate enhanced energetic particle fluxes in space. The only exception is related to the 09 June 2003 flare. We will discuss the origin of the weak particle event below (Section 4.3), but recall here that this is the only CME-less flare in the western hemisphere that was accompanied by a type II radio burst.

2.4. Summary of Observational Findings

- All GOES X class flares without CMEs show prominent microwave signatures of relativistic electron acceleration.
- The peculiar microwave signatures, such as high peak frequency and flux density, and on average a steep low-frequency spectrum, suggest gyrosynchrotron emission from compact sources in the low corona.
- The CME-less X class flares lack coronal radio emission at long decimetre and metre wavelengths, and DH type III bursts.
- Besides being CME-less, most of the flares have also no metric or DH type II burst. There are two exceptions: the events of 09 June 2003 and 16 July 2004 (13:49 UT) have metric type II bursts.
- While small SEP events would have been expected from the characteristics of the soft X-ray bursts, the only convincing SEP event with a CME-less flare was a weak event detected on 09 June 2003 by SoHO and ACE, but not by GOES.

3. Eruptive Events Following CME-Less Flares

3.1. Overview

On three occasions the CME-less X class flares were followed within a few hours by SEP events detected by GOES. Table 4 summarises properties of the SEP events. The start and peak times, as well as peak intensities, in the proton channels above 10 MeV are given in columns 2 – 4, together with the expected intensities (Equation (2)) in parentheses. The highest energy channel where the event was detected is given in column 5, with the peak

Table 4 SEP in eruptive flares following CME-less ones.

Flare	GOES protons			
	start	peak time	intensity (>10 MeV)	high energy extent
(1)	(2)	(3)	(4)	(5)
06 June 2000 14:58		08 June		
X2.3 N20 E14	∼22:20	∼10 UT	70 (38) pfu	100 MeV (<0.1 pfu)
02 April 2001 10:55				
X1.1 N16 W62	12:50	15:10	3 (22) pfu	100 MeV (<0.1 pfu)
15 January 2005 05:54				
M8.6 N11 E06	07:45	∼11 UT	8 (16) pfu	100 MeV (0.15 pfu)

Table 5 Radio emission and CME from eruptive flares following CME-less ones.

Microwaves		dm – m-λ	Type II	DH
CO(HF) [GHz]	Peak			
(1)	(2)	(3)	(4)	(5)
06 June 2000 14:58 (CME: 14:50 – 15:03 930 km s^{-1})				
>15	15:19/8.8 GHz/∼3000 sfu	IV	550X-30 MHz	IIIG, II
02 April 2001 10:55 (CME: 10:50 – 11:00 990 km s^{-1})				
>8.8	11:26/8.8 GHz/∼990 sfu	IV(M)	F/H 120 – 40 MHz	IIIG, II, IV
15 January 2005 05:54 (CME: 05:50 – 06:05 2050 km s^{-1})				
>15	06:30/5 GHz/3000 sfu	IV	∼150 – 18 MHz	IIIG, II, IV

intensity in parentheses. The intensities are given in particle flux units (pfu). They were not particularly strong. Only the first event was strong enough to be in the SEP event list at NOAA.[5] The late peak suggests that interplanetary shock acceleration dominated the proton flux above 10 MeV in this particular event, but during the three events GOES detected protons in its nominal channels above 100 MeV. All three SEP events can be associated with soft X-ray bursts from the same active region as the preceding CME-less flares. Characteristics of the soft X-ray bursts and the position of the associated flares, quoted from *Solar Geophysical Data – Comprehensive Reports*, are listed in the first column of Table 4.

All three events were accompanied by fast CMEs detected by SoHO/LASCO and listed in the CME catalogue. The onset times and speeds of the CMEs from the LASCO catalogue are summarised in Table 5, together with the radio properties (in the same format as Table 1). The CME liftoff times and speeds were inferred from the linear fit to the time – height trajectory, also provided by the LASCO catalogue. The two values of the liftoff time refer to the instants when the extrapolated trajectory projected to disk centre and 1 $R_\odot$, respectively. Table 5 further shows that while the frequency extent and peak flux density of the microwave spectra are similar to the CME-less flares, all three SEP-associated flares produced conspicuous emission at decimetre and longer wavelengths, including type IV and type II bursts,

[5] http://www.swpc.noaa.gov/ftpdir/indices/SPE.txt.

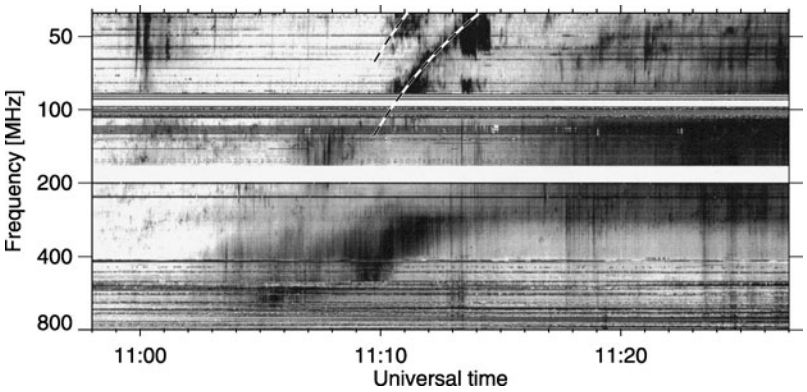

Figure 6 Dynamic radio spectrum (Astrophysikalisches Institut Potsdam; inverse colour scale: dark shading shows bright emission) of the eruptive event on 02 April 2001. The dashed lines show the fundamental and harmonic lanes, for the model of an exciter moving outward at speed 1630 km s^{-1} through a hydrostatically stratified plasma. The parameters of the model are: $T = 1.4$ MK, heliocentric distance of the harmonic level at 50 MHz 1.8 $R_\odot$.

and bright groups of type III bursts at decametre and longer waves. The peak frequencies of the microwave emission are lower than in the CME-less flares. In particular the 15 January 2005 microwave burst, for which detailed RSTN data were available, had a peak frequency well below those of the CME-less flares. The result is consistent with the relatively low peak frequency of CME-associated "gradual" microwave bursts reported by Cliver *et al.* (1986).

The SEP-associated eruptive flares hence underscore the characteristic properties of CME-less and SEP-less flares identified in the previous section, besides the absence of a CME: absence *vs.* presence of metric radio emission and DH type III bursts, steep *vs.* flat low-frequency microwave spectra, and high *vs.* moderate peak microwave frequencies. All these differences are consistent with confined particle populations in CME-less flares *vs.* particle populations able to escape to more extended coronal regions and interplanetary space.

In the following we illustrate the properties of one of these events, for which detailed radio spectrographic and imaging observations are available, and discuss the timing of the large-scale magnetic restructuring in the course of the CME and the initial release of electrons to interplanetary space.

3.2. The 02 April 2001 Event

The dynamic radio spectrum from dm-to-m waves during the first 30 min of the eruptive flare on 02 April 2001, 10:55 UT is shown in Figure 6. Several groups of bursts can be identified:

- A group of type III bursts in the 40 – 80 MHz range, starting at about 10:59 UT.
- The harmonic lane of a type II burst in the frequency range 90 – 40 MHz, between 11:10 UT (80 MHz) and 11:15 UT (40 MHz); the fundamental is visible between about 60 and 40 MHz. The backward extrapolation of the harmonic lane leads to a group of short and band-limited bursts between 170 and 130 MHz (11:06 UT). These bursts are a precursor of the type II burst, as defined by Klassen *et al.* (1999).

- A type IV burst, which started in the decimetre range (near 11:02 UT, 700 MHz). The high and low-frequency borders of this emission drift gradually to lower frequencies. Below 300 MHz the type IV emission brightened at 11:17 UT over an extended frequency range down to the 40 MHz border of the spectrograph.

The frequency drift rate of the type II burst can be used to infer an exciter speed. Proceeding like in Section 2.2.2 for the 09 June 2003 burst, we measure a relative drift rate $\frac{\mathrm{d}\ln\nu}{\mathrm{d}t} = -3.57 \times 10^{-3}\ \mathrm{s}^{-1}$. This implies for an exciter that travels outwards in an isothermal hydrostatic corona a speed $\upsilon_{\mathrm{II}} = 505\frac{T}{1.4\ \mathrm{MK}}(\frac{r_0}{R_\odot})^2\ \mathrm{km\,s}^{-1}$, where r_0 is the heliocentric distance where the drift rate was measured, *i.e.* of the source of harmonic emission at about 50 MHz. If we assume $r_0 = (1.5-2)R_\odot$, the exciter speed is about $\upsilon_{\mathrm{II}} = (1130-2010)\ \mathrm{km\,s}^{-1}$. It is well above the speed evaluated in the same way for the CME-less burst on 09 June 2003 (Section 2.2.2). The spectral lanes from one such model are overplotted on the dynamic spectrum in Figure 6.

The time history of the soft X-ray, decimetre – metre wave and decametre – hectometre wave emissions during the eruptive and the preceding CME-less flare is shown in Figure 7. The second and third panels from top display colour-coded 1D intensities (NRH data have been integrated over the solar south-north direction) in a plane where time is on the horizontal axis and the solar east-west direction, graded in solar radii, on the vertical axis. Yellow shading corresponds to the background, red to green-blue to bright emission. At 164 MHz (3rd panel from top) two noise storms, located at ($\sim$1.0 $\mathrm{R}_\odot$) and above the western limb ($\sim$1.5 $\mathrm{R}_\odot$), provided the dominant emission until 11 UT, including the time period of the CME-less flare. During the second flare starting 10:55 UT, the dominant emission at the two frequencies was the type IV burst with a delayed onset at the lower frequency. The radio sources underwent a systematic westward motion. This is a moving type IV burst (IV(M); Stewart, 1985; Pick, 1986), emitted by non thermal electrons in expanding loops or flux rope ("plasmoïd"), which is a non thermal manifestation of a CME or an eruptive prominence (see case studies in Gopalswamy and Kundu, 1989; Klein and Mouradian, 2002; Claßen *et al.*, 2003; Vršnak *et al.*, 2003; Pick *et al.*, 2005; Raoult-Barbezat and Klein, 2005).

At decametre and longer wavelengths (two bottom panels of Figure 7) the event started with a bright group of DH type III bursts. They are the low-frequency continuation of the type III bursts observed in the 40 – 80 MHz range in Potsdam. The DH type III bursts were followed by a broadband emission in the 14 – 5 MHz range, starting near 11:25 UT. This is either the low-frequency extension of the type IV burst or a type II burst, which at these frequencies is generally attributed to the CME shock. The existence of drifting lanes suggests the type II interpretation, while the broad overall bandwidth is more reminiscent of a type IV burst.

The type III bursts at long metric and longer waves (frequency below about 80 MHz) occurred during the early rise of the soft X-ray emission, before the start of the type IV burst at 327 MHz and lower frequencies. The early flare-related energy release and the access of particles to open coronal flux tubes hence occurred at the time of the early acceleration of the CME. It is unlikely that the CME already caused a major restructuring of the large-scale coronal magnetic field connected with the flaring active region so early. The timing rather suggests that energetic particles escaped through the corona along pre-existing open magnetic field lines.

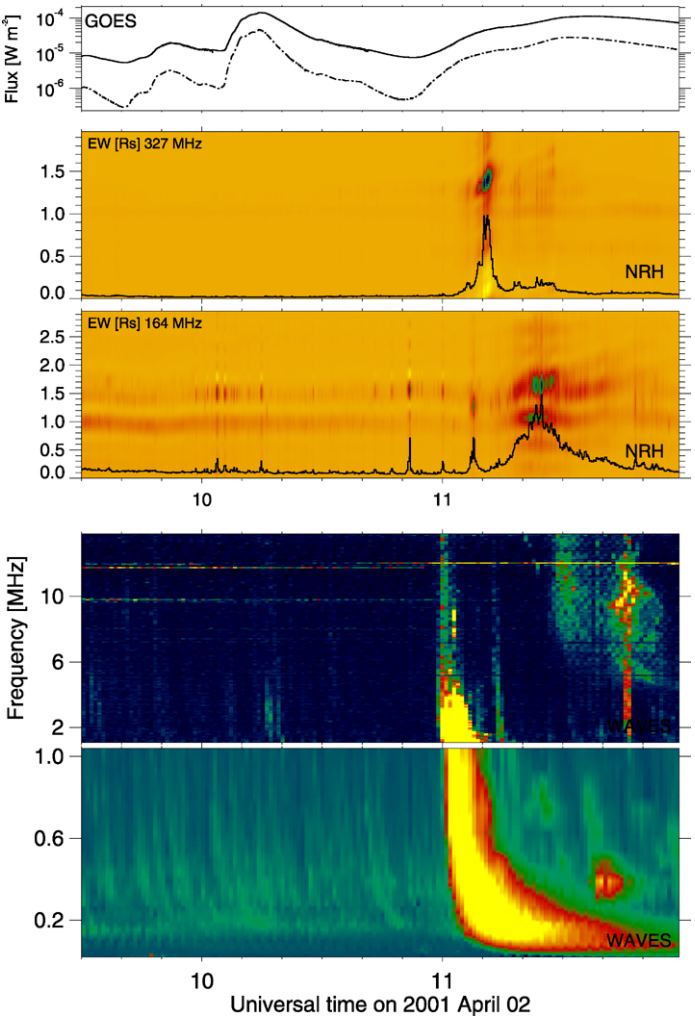

Figure 7 Time history of the soft X-ray (top panel; GOES), decimetre-to-metre wave (middle; NRH) and decametre-to-hectometre (DH) wave emission (bottom; *Wind*/WAVES) around the CME-less GOES X class flare on 02 April 2001 10:04 UT and the subsequent eruptive flare/CME at 10:55 UT. The NRH observations are represented as colour-coded intensities (from yellow for the background to green-blue for the brightest emission) as a function of time and the solar east – west coordinate, graded in units of a solar radius. Zero is at the centre of the disk. Only the western solar hemisphere is shown.

4. Discussion and Conclusions

4.1. CME-Less Flares and the Confinement of Energetic Particles

CME-less flares are generally referred to as 'confined'. The absence of CMEs in these events was related by Wang and Zhang (2007) to the location of energy release. These authors analysed the magnetic field configuration in the neighbourhood of the energy release site in the low corona and in the overlying corona, dominated by the magnetic structures that surround the energy release region. They showed that during CME-less flares the energy

release region, as inferred from the EUV flare brightenings, is closer to the centre of the magnetic flux concentration in the parent AR, and has relatively more overlying magnetic flux, than during eruptive flares. This justifies the term 'confined' flare for the CME-less events.

This picture of confinement is corroborated by the radio observations presented here: the steep low-frequency spectra of the microwave bursts, the absence of emission at decimetre-to-metre wavelengths at the time of the microwave bursts, and the absence of DH type III bursts, which would have shown the escape of electrons to the high corona and interplanetary space, will all be expected if the flare-accelerated electrons are confined in compact structures in the low corona.

The statement on the absence of DH type III bursts may be ambiguous, when it relies on the distinction of flare-related DH type III bursts and storm type III bursts. We illustrate this for the 02 April 2001 flares in Figure 7. The slightly enhanced background (light green) of the low-frequency channel of WAVES plotted in the bottom panel represents an uninterrupted series of faint storm type III bursts. The storm is clearly not related with any of the two flares in the plotted time window, but accompanies the two noise storms seen in the 164 MHz NRH record (3rd panel from top). The brighter type III burst near 10:15 UT occurred near the maximum of the CME-less soft X-ray burst, and might be identified as flare-related. It would then have to be considered as a "late" event in Table 1, and would not contradict our earlier conclusion on the confinement of the flare-accelerated electrons. But the type III burst occurs at the time of bursty emission at 164 MHz. The 164 MHz burst is strongly circularly polarised (80 – 90%), and its source is far above the western limb. The 164 MHz burst is hence part of the noise storm. We also note that this peculiar DH type III burst is brighter than others in the high-frequency window of WAVES (1 – 14 MHz), but not in the low-frequency one. So there are several pieces of evidence that show this DH type III burst to be associated with the noise storm rather than with the CME-less flare. We did not find similar ambiguities in other events, and therefore believe that there is no confusion between flare-related DH type III bursts and storm type III bursts in our analysis.

4.2. CME-Less *vs.* Eruptive Flares: Particle Acceleration and Access to Interplanetary Space

CME-less flares turn out to be in general efficient electron accelerators, as shown by the bright microwave bursts. These electrons, and most probably protons accelerated together with them, do not produce SEP events, because they remain confined in the low corona. Indeed no SEP event was observed by GOES even from the confined flares in the western solar hemisphere, where accelerated particles, if they escaped to the high corona, would usually be expected to be detected by spacecraft near Earth. The weak energetic particle flux enhancements seen at SoHO and ACE in one event associated with a type II burst will be discussed in Section 4.3.

The comparison of the SEP-less confined flares with SEP-producing eruptive ones occurring a few hours later in the same active region corroborates the basic difference in terms of particle confinement: the eruptive flares had prominent dm-m wave emission and groups of bright DH type III bursts. The associated SEP events were clearly detected by GOES, even if the particle intensity was weak. This confirms the fact that flares, CMEs, metre wave type IV bursts and bright groups of DH type III bursts are necessarily associated with major SEP events, as observed by GOES, in line with earlier findings by Kahler (1982) for the type IV bursts and Cane, Erickson, and Prestage (2002) and MacDowall *et al.* (2003) for the DH type III bursts. The situation is not the same for impulsive SEP events, which may occur

without type IV emission, as shown in Klassen *et al.* (2002), Maia and Pick (2004), Klein *et al.* (2005) and Klein and Posner (2005). The presence of type III bursts signals primarily that particles accelerated near the flare site reach magnetic flux tubes that are open to the high corona.

It is tempting to conclude from the association of SEP with eruptive flares that the CME is necessary to open the coronal magnetic field and give the particles access to interplanetary space. An example for this interpretation was discussed by Démoulin *et al.* (2007). But this may not be the adequate interpretation in the cases discussed in the present paper, because the DH type III bursts started during the impulsive phase of the eruptive flares, when the CME probably did not yet have the time to re-organise the large-scale coronal magnetic field connected to the flare site. An alternative interpretation is that CMEs and type III bursts occur under similar conditions: CMEs are more probable when energy is released at the periphery of an active region (Wang and Zhang, 2007), and the same condition was established for type III bursts at metre wavelengths (Axisa, 1974; Zlobec *et al.*, 1990; Hofmann and Ruždjak, 2007). This suggests that even if large-scale open magnetic flux tubes exist in active regions hosting confined flares, particles are accelerated too far from them and are unable to reach them.

4.3. CME-Less Flares and Type II Bursts

Two out of the 15 CME-less flares were accompanied by metric type II bursts, while no type II emission at decametric or longer wavelengths was detected by *Wind*/WAVES. Although it is not the subject of the present paper, we briefly address the relevance of this finding to the understanding of the shock waves that generate metre wave type II bursts. We believe that these two flares are not just misidentifications. Indeed both flares share most of the observational indications of confinement of the flare-accelerated electrons with the whole set of events, especially the absence of type IV emission at dm – m waves and of DH type III bursts during the impulsive flare phase. We therefore consider that the occurrence of metric type II bursts with CME-less flares is a significant, albeit rare, feature.

CME-less X class flares are cases where a pure blast wave shock, if it existed in the corona, could be observed. The high soft X-ray flux of the studied flares suggests that a major energy release occurred, and the impulsive rise tells us that energy was released rapidly. The fact that type II bursts were only detected in two out of 15 events confirms that, if ever, shocks are rarely generated as pure blast waves. We also emphasise that coronal shocks may be related to drivers, revealed by expanding soft X-ray structures, on smaller spatial scale than CMEs (Klein *et al.*, 1999). The problem of the origin of coronal (metre wavelengths) type II shocks that produce metric type II bursts has been discussed elsewhere (see Vršnak and Cliver, 2008; Nindos *et al.*, 2008 and references therein).

It is worth emphasising that the only CME-less flare on the western hemisphere that was clearly associated with an increase of the intensities of relativistic electrons and low-energy protons in space also produced a metric type II burst. Our estimation of the exciter speed and Mach number shows that the shock was weak, but the well-defined type II emission demonstrates that it accelerated radio-emitting electrons. The detection of weak fluxes of electrons up to relativistic energies and of MeV protons by particle instruments aboard SoHO and ACE agrees with earlier results reported from the timing of type II bursts and electron releases (Hucke, Kallenrode, and Wibberenz, 1992; Klassen *et al.*, 2002; Kahler *et al.*, 2007), although the interpretation may be equivocal (Cane, Erickson, and Prestage, 2002; Kahler, 2007). The only available quantitative estimate of electron numbers accelerated at a coronal type II shock (Klein *et al.*, 2003) implies that metric type II shocks are poor electron accelerators in the corona, but the constraints are still consistent with moderate electron

events in space. Therefore the shock provides a plausible explanation for the origin of the weak SEP event on 09 June 2003.

4.4. Soft X-ray Bursts and SEP Forecasting

The present result has potential importance in the forecasting of SEP events. Despite the widespread belief that large SEP events result from particle acceleration at CME shocks, soft X-ray burst characteristics play an important part in operational models used for SEP forecasting (Garcia, 2004; Balch, 2008). Indeed Belov *et al.* (2007) showed that the probability of an SEP event rises with the peak soft X-ray flux of the flare. But they also demonstrated (their Figure 3) that more than 30% of GOES X class flares westward of longitude E 20° have no SEP event associated with them. Our result gives a simple physical explanation in terms of particle confinement in the corona for at least a fraction of these events. The absence of dm – m wave radiation and of type III bursts at decametric and longer waves also provides an easy-to-use observational tool to identify these specific events in real time.

Acknowledgements The SOHO/COSTEP project is supported under grant 50 OC 0902 by the German Bundesministerium für Wirtschaft through the Deutsches Zentrum für Luft- und Raumfahrt (DLR). SoHO is a project of international cooperation between ESA and NASA. The Nançay Radio Observatory is funded by the French Ministry of Education, the CNRS, and the Région Centre. This work benefited from the data of other space borne and ground based observatories: the ACE and GOES spacecraft (data provided through the ACE Science Center, The National Geophysical Data Center NGDC/NOAA and the Solar Data Analysis Center at NASA/GSFC), the solar radio observatories at Athens (ARTEMIS), Culgoora, Green Bank (GBS-BRS), Hiraiso, Nobeyama, Potsdam (OSRA Tremsdorf), Zurich (Phoenix) and the Radio Telescope Network of the US Air Force (RSTN, data provided through NGDC), the *Wind*/WAVES experiment, as well as the Radio monitoring web page, generated and maintained at Observatoire de Paris, Meudon, by LESIA/UMR CNRS 8109 in cooperation with the Artemis team, Universities of Athens and Ioannina and the Naval Research Laboratory. Extensive use was made of the SoHO/LASCO CME catalogue, generated and maintained at the CDAW Data Center by NASA and The Catholic University of America in cooperation with the Naval Research Laboratory. KLK acknowledges helpful discussions with P. Démoulin, N. Vilmer, J. Zhang and at the International Space Science Institute (ISSI) in Bern, within the project "Transport of energetic particles in the inner heliosphere" led by W. Droege. The authors acknowledge helpful comments by the referee.

References

Axisa, F.: 1974, On the role of the magnetic configuration of flares for production of type III solar radio bursts. *Solar Phys.* **35**, 207 – 224.

Balch, C.C.: 2008, Updated verification of the Space Weather Prediction Center's solar energetic particle prediction model. *Space Weather* **6**, S01001.

Belov, A., Kurt, V., Mavromichalaki, H., Gerontidou, M.: 2007, Peak-size distributions of proton fluxes and associated soft X-ray flares. *Solar Phys.* **246**, 457 – 470.

Benz, A.O., Güdel, M.: 1994, The soft X-ray/microwave ratio of solar and stellar flares and coronae. *Astron. Astrophys.* **285**, 621 – 630.

Bewsher, D., Harrison, R.A., Brown, D.S.: 2008, The relationship between EUV dimming and coronal mass ejections. I. Statistical study and probability model. *Astron. Astrophys.* **478**, 897 – 906.

Bougeret, J.L., Kaiser, M.L., Kellogg, P.J., Manning, R., Goetz, K., Monson, S.J., Monge, N., Friel, L., Meetre, C.A., Perche, C., Sitruk, L., Hoang, S.: 1995, Waves: The radio and plasma wave investigation on the *Wind* spacecraft. *Space Sci. Rev.* **71**, 231 – 263.

Cane, H.V., Erickson, W.C., Prestage, N.P.: 2002, Solar flares, type III radio bursts, coronal mass ejections and energetic particles. *J. Geophys. Res.* **107**, 1315.

Caroubalos, C., Maroulis, D., Patavalis, N., Bougeret, J., Dumas, G., Perche, C., Alissandrakis, C., Hillaris, A., Moussas, X., Preka-Papadema, P., Kontogeorgos, A., Tsitsipis, P., Kanelakis, G.: 2001, The new multichannel radiospectrograph ARTEMIS-IV/HECATE, of the University of Athens. *Exp. Astron.* **11**, 23 – 32.

Chertok, I.M.: 1990, On the correlation between the solar gamma-ray line emission, radio bursts and proton fluxes in the interplanetary space. *Astron. Nachr.* **311**, 379 – 381.

Claßen, H.T., Mann, G., Klassen, A., Aurass, H.: 2003, Relative timing of electron acceleration and injection at solar flares: A case study. *Astron. Astrophys.* **409**, 309 – 316.

Cliver, E.W., Dennis, B.R., Kiplinger, A.L., Kane, S.R., Neidig, D.F., Sheeley, N.R., Koomen, M.J.: 1986, Solar gradual hard X-ray bursts and associated phenomena. *Astrophys. J.* **305**, 920 – 935.

Correia, E., Kaufmann, P., Magun, A.: 1994, The observed spectrum of solar burst continuum emission in the submillimeter spectral range. In: *IAU Symp. 154: Infrared Solar Physics*, 125 – 129.

Dauphin, C., Vilmer, N., Krucker, S.: 2006, Observations of a soft X-ray rising loop associated with a type II burst and a coronal mass ejection in the 03 November 2003 X-ray flare. *Astron. Astrophys.* **455**, 339 – 348.

Démoulin, P., Klein, K.L., Goff, C.P., van Driel-Gesztelyi, L., Culhane, J.L., Mandrini, C.H., Matthews, S.A., Harra, L.K.: 2007, Decametric N burst: A consequence of the interaction of two coronal mass ejections. *Solar Phys.* **240**, 301 – 313.

Dulk, G.A.: 1985, Radio emission from the sun and stars. *Annu. Rev. Astron. Astrophys.* **23**, 169 – 224.

Fürst, E.: 1971, A statistical research on solar microwave bursts. *Solar Phys.* **18**, 84 – 86.

Garcia, H.A.: 2004, Forecasting methods for occurrence and magnitude of proton storms with solar soft X-rays. *Space Weather* **2**, S02002.

Gergely, T.E., Kundu, M.R., Hildner, E.: 1983, A coronal transient associated with a high-speed type II burst. *Astrophys. J.* **268**, 403 – 411.

Gergely, T.E., Kundu, M.R., Erskine, F.T. III, Sawyer, C., Wagner, W.J., Illing, R., House, L.L., McCabe, M.K., Stewart, R.T., Nelson, G.J.: 1984, Radio and visible-light observations of a coronal arcade transient. *Solar Phys.* **90**, 161 – 176.

Gold, R.E., Krimigis, S.M., Hawkins, S.E., Haggerty, D.K., Lohr, D.A., Fiore, E., Armstrong, T.P., Holland, G., Lanzerotti, L.J.: 1998, Electron, proton, and alpha monitor on the *Advanced Composition Explorer* spacecraft. *Space Sci. Rev.* **86**, 541 – 562.

Gopalswamy, N., Kundu, M.R.: 1989, A slowly moving plasmoid associated with a filament eruption. *Solar Phys.* **122**, 91 – 110.

Gopalswamy, N., Akiyama, S., Yashiro, S.: 2009, Major solar flares without coronal mass ejections. In: Gopalswamy, N., Webb, D.F. (eds.) *Universal Heliophysical Processes*, *IAU Symp.* **257**, 283 – 286.

Gopalswamy, N., Yashiro, S., Krucker, S., Stenborg, G., Howard, R.A.: 2004, Intensity variation of large solar energetic particle events associated with coronal mass ejections. *J. Geophys. Res.* **109**, A12105.

Guidice, D.A., Castelli, J.P.: 1975, Spectral distributions of microwave bursts. *Solar Phys.* **44**, 155 – 172.

Hofmann, A., Ruždjak, V.: 2007, Favourable magnetic field configurations for generation of flare-associated meter-wave type III radio bursts. *Solar Phys.* **240**, 107 – 119.

Hucke, S., Kallenrode, M.B., Wibberenz, G.: 1992, Interplanetary type III radiobursts and relativistic electrons. *Solar Phys.* **142**, 143 – 155.

Jin, M., Ding, M.D., Chen, P.F., Fang, C., Imada, S.: 2009, Coronal mass ejection induced outflows observed with Hinode/EIS. *Astrophys. J.* **702**, 27 – 38.

Kahler, S.W.: 1982, Radio burst characteristics of solar proton flares. *Astrophys. J.* **261**, 710 – 719.

Kahler, S.W.: 2001, The correlation between solar energetic particle peak intensities and speeds of coronal mass ejections: Effects of ambient particle intensities and energy spectra. *J. Geophys. Res.* **106**, 20947 – 20956.

Kahler, S.W.: 2007, Solar sources of heliospheric energetic electron events – shocks or flares? *Space Sci. Rev.* **129**, 359 – 390.

Kahler, S.W., Aurass, H., Mann, G., Klassen, A.: 2007, Solar radio burst and solar wind associations with inferred near-relativistic electron injections. *Astrophys. J.* **656**, 567 – 576.

Kai, K., Melrose, D.B., Suzuki, S.: 1985, Storms. In: McLean, D., Labrum, N. (eds.) *Solar Radiophysics: Studies of Emission from the Sun at Metre Wavelengths*, Cambridge University Press, Cambridge, 415 – 441.

Kayser, S.E., Bougeret, J., Fainberg, J., Stone, R.G.: 1987, Comparisons of interplanetary type III storm footpoints with solar features. *Solar Phys.* **109**, 107 – 118.

Kerdraon, A., Delouis, J.: 1997, The Nançay radioheliograph. In: Trottet, G. (ed.) *Coronal Physics from Radio and Space Observations*, *Lecture Notes in Physics* **483**, Springer, Berlin, 192 – 201.

Klassen, A., Aurass, H., Klein, K.L., Hofmann, A., Mann, G.: 1999, Radio evidence on shock wave formation in the solar corona. *Astron. Astrophys.* **343**, 287 – 296.

Klassen, A., Bothmer, V., Mann, G., Reiner, M.J., Krucker, S., Vourlidas, A., Kunow, H.: 2002, Solar energetic electron events and coronal shocks. *Astron. Astrophys.* **385**, 1078 – 1088.

Klein, K.L., Mouradian, Z.: 2002, The dynamics of an erupting prominence. *Astron. Astrophys.* **381**, 683 – 693.

Klein, K.L., Posner, A.: 2005, The onset of solar energetic particle events: prompt release of deka-MeV protons and associated coronal activity. *Astron. Astrophys.* **438**, 1029 – 1042.

Klein, K.L., Trottet, G., Vilmer, N.: 2009, A search for solar energetic particle events with CME-less flares. In: *Proc. 31st ICRC*, Paper 0634. http://icrc2009.uni.lodz.pl/proc/pdf/icrc0634.pdf.

Klein, K.L., Khan, J.I., Vilmer, N., Delouis, J., Aurass, H.: 1999, X-ray and radio evidence on the origin of a coronal shock wave. *Astron. Astrophys.* **346**, L53 – L56.

Klein, K.L., Schwartz, R.A., McTiernan, J.M., Trottet, G., Klassen, A., Lecacheux, A.: 2003, An upper limit of the number and energy of electrons accelerated at an extended coronal shock wave. *Astron. Astrophys.* **409**, 317 – 324.

Klein, K.L., Krucker, S., Trottet, G., Hoang, S.: 2005, Coronal phenomena at the onset of solar energetic electron events. *Astron. Astrophys.* **431**, 1047 – 1060.

Koutchmy, S.: 1994, Coronal physics from eclipse observations. *Adv. Space Res.* **14**(4), 29 – 39.

Lecacheux, A.: 2000, The Nançay Decameter Array: A useful step towards giant, new generation radio telescopes for long wavelength radio astronomy. In: Stone, R., Weiler, K., Goldstein, M., Bougeret, J.L. (eds.) *Radio Astronomy at Long Wavelengths*, *AGU Monograph* **119**, 321 – 328.

MacDowall, R.J., Lara, A., Manoharan, P.K., Nitta, N.V., Rosas, A.M., Bougeret, J.L.: 2003, Long-duration hectometric type III radio bursts and their association with solar energetic particle (SEP) events. *Geophys. Res. Lett.* **30**(12), 120000-1.

Maia, D., Pick, M.: 2004, Revisiting the origin of impulsive electron events: coronal magnetic restructuring. *Astrophys. J.* **609**, 1082 – 1097.

Mann, G., Classen, T., Aurass, H.: 1995, Characteristics of coronal shock waves and solar type II radio bursts. *Astron. Astrophys.* **295**, 775 – 781.

Mann, G., Aurass, H., Voigt, W., Paschke, J.: 1992, Preliminary observations of solar type II bursts with the new radiospectrograph in Tremsdorf (Germany). In: *Coronal Streamers, Coronal Loops, and Coronal and Solar Wind Composition* **SP-348**, ESA, Noordwijk, 129 – 132.

Marqué, C., Posner, A., Klein, K.L.: 2006, Solar energetic particles and radio-silent fast coronal mass ejections. *Astrophys. J.* **642**, 1222 – 1235.

Messmer, P., Benz, A.O., Monstein, C.: 1999, PHOENIX-2: A new broadband spectrometer for decimetric and microwave radio bursts first results. *Solar Phys.* **187**, 335 – 345.

Müller-Mellin, R., Kunow, H., Fleissner, V., Pehlke, E., Rode, E., Roschmann, N., Scharmberg, C., Sierks, H., Rusznyak, P., McKenna-Lawlor, S., Elendt, I., Sequeiros, J., Meziat, D., Sanchez, S., Medina, J., del Peral, L., Witte, M., Marsden, R., Henrion, J.: 1995, COSTEP – Comprehensive Suprathermal and Energetic Particle Analyser. *Solar Phys.* **162**, 483 – 504.

Nakajima, H., Sekiguchi, H., Sawa, M., Kai, K., Kawashima, S.: 1985, The radiometer and polarimeters at 80, 35, and 17 GHz for solar observations at Nobeyama. *Publ. Astron. Soc. Japan* **37**, 163 – 170.

Nelson, G.J., Robinson, R.D.: 1975, Multi-frequency heliograph observations of type II bursts. *Proc. Astron. Soc. Australia* **2**, 370 – 373.

Nindos, A., Aurass, H., Klein, K.L., Trottet, G.: 2008, Radio emission of flares and coronal mass ejections. *Solar Phys.* **253**, 3 – 41.

Nita, G.M., Gary, D.E., Lee, J.: 2004, Statistical study of two years of solar flare radio spectra obtained with the Owens Valley Solar Array. *Astrophys. J.* **605**, 528 – 545.

Pacholczyk, A.G.: 1970, *Radio Astrophysics*, Freeman, San Francisco.

Pick, M.: 1986, Observations of radio continua and terminology. *Solar Phys.* **104**, 19 – 32.

Pick, M., Démoulin, P., Krucker, S., Malandraki, O., Maia, D.: 2005, Radio and X-ray signatures of magnetic reconnection behind an ejected flux rope. *Astrophys. J.* **625**, 1019 – 1026.

Priest, E.R.: 1982, *Solar Magneto-hydrodynamics*, Reidel, Dordrecht.

Raoult-Barbezat, A., Klein, K.: 2005, A coronal mass ejection on 05 February 2005: Radio, EUV and visible light observations. In: *The Dynamic Sun: Challenges for Theory and Observations*, *ESA SP* **600**.

Robbrecht, E., Patsourakos, S., Vourlidas, A.: 2009, No trace left behind: STEREO observation of a coronal mass ejection without low coronal signatures. *Astrophys. J.* **701**, 283 – 291.

Spangler, S.R., Shawhan, S.D.: 1974, Short duration solar microwave bursts and associated soft X-ray emission. *Solar Phys.* **37**, 189 – 203.

Stewart, R.T.: 1985, Moving Type IV bursts. In: McLean, D., Labrum, N. (eds.) *Solar Radiophysics: Studies of Emission from the Sun at Metre Wavelengths*, Cambridge University Press, Cambridge, 361 – 383.

Vršnak, B., Cliver, E.W.: 2008, Origin of coronal shock waves. *Solar Phys.* **253**, 215 – 235.

Vršnak, B., Aurass, H., Magdalenić, J., Gopalswamy, N.: 2001, Band-splitting of coronal and interplanetary type II bursts. I. Basic properties. *Astron. Astrophys.* **377**, 321 – 329.

Vršnak, B., Klein, K.L., Warmuth, A., Otruba, W., Skender, M.: 2003, Vertical dynamics of the energy release process in a simple two-ribbon flare. *Solar Phys.* **214**, 325 – 338.

Wang, Y., Zhang, J.: 2007, A comparative study between eruptive X-class flares associated with coronal mass ejections and confined X-class flares. *Astrophys. J.* **665**, 1428 – 1438.

White, S.M.: 2007, Solar radio bursts and space weather. *Asian J. Phys.* **16**, 189.

Yashiro, S., Gopalswamy, N., Michalek, G., St. Cyr, O.C., Plunkett, S.P., Rich, N.B., Howard, R.A.: 2004, A catalog of white light coronal mass ejections observed by the SOHO spacecraft. *J. Geophys. Res.* **109**(A18), A07105.

Yashiro, S., Michalek, G., Akiyama, S., Gopalswamy, N., Howard, R.A.: 2008, Spatial relationship between solar flares and coronal mass ejections. *Astrophys. J.* **673**, 1174 – 1180.

Zlobec, P., Messerotti, M., Ruzdjak, V., Vrsnak, B., Karlicky, M.: 1990, The role of the magnetic field intensity and geometry in the type III burst generation. *Solar Phys.* **130**, 31 – 37.